DALTON
FULL PAPER

Synthesis, electrical properties and crystal structure of a new radical-ion salt based on π-extended bis(TTF) and a Keggin heteropolymolybdate

Jun Peng,[a] Enbo Wang,*[a] Yunshan Zhou,[a] Yan Xing,[b] Hengqing Jia,[b] Yonghua Lin[b] and Yongjia Shen[c]

[a] *Department of Chemistry, Northeast Normal University, Changchun, 130024, P.R.China*
[b] *Changchun Institute of Applied Chemistry, Chinese Academy of Science, Changchun, 130022, P.R. China*
[c] *Institute of Fine Chemicals, East China University of Science and Technology, Shanghai, 200237, P.R. China*

Received 29th June 1998, Accepted 23rd September 1998

By electrocrystallization of 2,6-[4,5-bis(*n*-butylsulfanyl)-1,3-dithiol-2-ylidene]-4,8-bis(6-iodo-*n*-hexyloxy)-1,3,5,7-tetrathia-s-indacene (BHBDTI) and $[NBu_4]_4[SiMo_{12}O_{40}]$ in the mixed solvent $CHCl_2CH_2Cl$ and CH_3CN, the new radical-ion salt $[C_{42}H_{60}Cl_2O_2S_{12}]_2[SiMo_{12}O_{40}]$ was prepared. It was characterized by means of IR and ESR spectroscopy and X-ray diffraction. In the crystal structure, organic radical dications and silicomolybdate anions are alternatively arranged along the *a* axis to form a 1-D conducting layer. The organic layer consists of two isolated groups of BHBDTI divided by the (011) plane without short interatomic contacts. However, in each group, BHBDTI molecules associate with each other in a head to tail manner running along the [011] direction and face-to-face overlapping with a relative shift by approximately one TTF subunit along the long axis of the molecule and a slight shift along the short axis of the molecule with significantly short S · · · S contacts. The room-temperature d.c. conductivity determined by the two-probe method is 10^{-4} S cm^{-1}, suggesting that the compound is a semiconductor.

Polyoxometalates are versatile in many aspects,[1] and new efforts have been made to explore their applications in fields such as catalysis, molecular materials, non-linear optical materials and liquid crystals.[2] All these reflect a current interest in combining different inorganic and organic moieties by molecular assemblies to produce hybrid materials, which open up broad prospects for the old chemistry.

Radical-cation and charge-transfer salts containing TTF have attracted much interest since the discovery of conductivity of the TTF–TCNQ charge-transfer (CT) complex.[3] In recent years, dozens, if not hundreds, of TTF derivatives as donors have been combined with various acceptors ranging from small closed-shell anions to large polyoxometalate clusters. Hundreds of synthetic metals consisting of such organic–inorganic moieties have been explored, of which many exhibit not only metallic behavior but also superconductivity.[4,5] It is believed that the electrical properties of radical-cation and charge-transfer salts containing TTF critically depend on the stabilization of a chalcogen–chalcogen network which must be built in more than one dimension. Thus many efforts have been made to search for new extended donors.[6]

The strategy which consists of associating TTF-like donor molecules and heteropolyanions has been explored by a number of different groups.[7–10] However, most of the hybrid compounds are semiconductors, except for $[BEDT\text{-}TTF]_{11}[P_2W_{18}O_{62}]$[11] and $(BEDT\text{-}TTF)_5VW_5O_{19}$ [BEDT = bis(ethylenedithio)].[12] The former is metallic at room temperature (r.t.) and exhibits a metal–semiconductor transition at 220–230 K. The latter exhibits metallic behaviour down to 250 K where a metal–insulator transition occurs.

We report here the synthesis, electrical properties and crystal structure of a new radical-cation salt based on a π-extended bis(TTF) cation and a big inorganic anion, $[C_{42}H_{60}Cl_2O_2S_{12}]_2[SiMo_{12}O_{40}]$, the first example of radical-cation salt of bis(TTF) possessing a central benzene subunit with heteropolymolybdate.

Results and discussion

Preparation

As is known, all "dimeric" TTF with connecting π bonds can donate twice as many electrons as the "mono" TTF, and there are strong stabilizing effects for the second redox step of the "dimeric" TTF yielding a dication.[6] The dication can be generated either by chemical or by electrochemical oxidation of a neutral molecule.[13] In the present radical salt, dications of the donor were produced electrochemically and assembled with heteropolyanion. It is noted that the crystal structure determination shows chloro-*n*-hexyloxy groups present in the organic donor molecule, $C_{42}H_{60}Cl_2O_2S_{12}$ (denoted as BHBDTI), while the starting material used is $C_{42}H_{60}I_2O_2S_{12}$. A substitution reaction between chlorine and iodine atoms occurs during the electrocrystallization. This is possible because of the presence of $CHCl_2CH_2Cl$ which is used as a solvent. Another point is that adding more than several drops of water seems important for growing single crystals of good quality.

The crystal structure

(a) $[SiMo_{12}O_{40}]^{4-}$. The unit cell contains an independent silicomolybdate anion located at an inversion centre. The polyoxoanion shows the same type of crystallographic disorder as has been found in many other crystal structures with the Keggin anions, which has been explained by several arguments [14–18] and will not be discussed here. The central Si atom is surrounded by a cube of eight oxygen atoms, with each oxygen site half-occupied, and the Mo atoms situated at the corners of a regular cubooctahedron. All Mo–Mo distances are equal. The Mo–O (terminal) bond lengths are in the usual range of 1.602–1.672 Å, whereas the Mo–O–Mo bonds in all MoO_6 octahedra fall into two well resolved categories: the long pairs of Mo–O bonds in the range 1.990–2.062 Å and the short pairs of Mo–O bonds 1.753–1.838 Å with the two Mo–O bonds in a pair being

Table 1 Comparison of bond distances (Å) and angles (°) in $[SiMo_{12}O_{40}]^{4-}$ *

	1	2	3	4	
$Mo–O_{b/c}$ (l)	1.990–2.062	1.970–1.979	1.93–1.98	—	
	(0.072)	(0.009)	(0.05)	—	
	[2.022]	[1.975]	[1.958]	[1.957]	
$Mo–O_{b/c}$ (s)	1.753–1.838	1.769–1.828	1.79–1.84	—	
	(0.085)	(0.059)	(0.05)	—	
	[1.791]	[1.798]	[1.826]	[1.853]	
$\Delta Mo–O_{b/c}$ (l − s)	0.231	0.177	0.132	0.104	
$Mo–O_{b/c}–Mo$	131.4–138.3	135.9–140.1	—	118.80–121.56	148.51–153.66
	(6.9)	(4.2)	—	—	(5.15)
	[136.2]	[138.5]	—	[120.5]	[151.3]

( ), Differences; [ ], averages. * All the structures of the anions have the same kind of disorder except for the last one which is a normal Keggin structure without disorder: $[C_{42}H_{60}Cl_2O_2S_{12}]_2[SiMo_{12}O_{40}]$ **1** (this work), $[C_{10}H_8S_8]_8[SiMo_{12}O_{40}]\cdot 10H_2O$[19] **2**, $[Fe(C_5Me_5)_2]_4[SiMo_{12}O_{40}]\cdot DMF$[14] **3** and $[CH_6N_3]_4[SiMo_{12}O_{40}]\cdot H_2O$ **4**.[20]

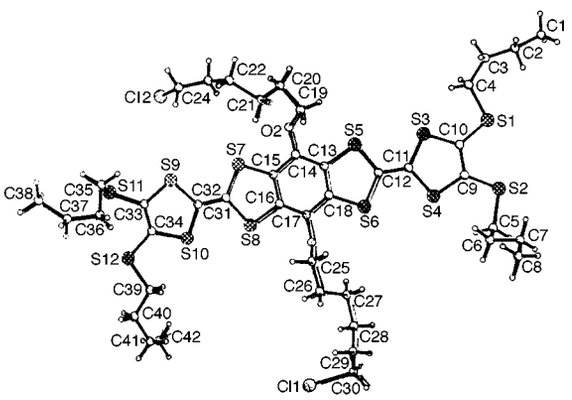

Fig. 1 Molecular structure of $C_{42}H_{60}Cl_2O_2S_{12}$ (denoted BHBDTI) with atom numbering.

in the *cis* positions. The mean bond order for the long ones is 0.7, and for the short ones 1.3. Angles Mo–O–Mo are in the range of 131.4–138.3°.

It is interesting to compare bond lengths and angles for this title compound with those for some other silicomolybdates[19,20] (see Table 1). As shown in Table 1, the increasing order of the mean bond length of the long (l) $Mo–O_{b/c}$ bonds [$Mo–O_{b/c}$ (l)] for four compounds is $CH_6N_3–SiMo_{12} < Fe(C_5Me_5)_2–SiMo_{12} < C_{10}H_8S_8–SiMo_{12} < C_{42}H_{60}Cl_2O_2S_{12}–SiMo_{12}$ whereas the mean bond lengths of the short (s) $Mo–O_{b/c}$ bonds [$Mo–O_{b/c}$ (s)] are in the reverse order $CH_6N_3–SiMo_{12} > Fe(C_5Me_5)_2–SiMo_{12} > C_{10}H_8S_8–SiMo_{12} > C_{42}H_{60}Cl_2O_2S_{12}–SiMo_{12}$, *i.e.* the distortion of MoO_6 octahedra in the present compound is the greatest. It seems that the extent of distortion is roughly parallel to the volumes of the organic molecules and their hydrophobicity.

(b) BHBDTI. In the unit cell the BHBDTI molecule is nearly planar except for the alkyl and alkyloxy side-chains. The distances among the terminal atoms of the molecule are C(1)···C(8) 10.322 Å, C(38)···C(42) 9.623 Å, Cl(1)···C(42) 7.873 and Cl(2)···C(38) 7.475 Å. The mean C–C and C–S bond lengths of the π system (1.39 and 1.73 Å) are 0.07 and 0.05 Å shorter than the corresponding ones of the branch chains (1.46 and 1.78 Å), respectively. The bond lengths of the TTF subunit given in Table 2 are in agreement with those of the BEDT-TTF compounds with formal fractional charge.[19] The molecular structure with atom numbering is shown in Fig.1.

(c) $[C_{42}H_{60}Cl_2O_2S_{12}]_2[SiMo_{12}O_{40}]$. The X-ray structural analysis gives a ratio BHBDTI : $SiMo_{12}O_{40}^{4-} = 2:1$, a reasonable result in terms of the charge balance of the salt. The BHBDTI molecules are stacked face to face to form an organic layer along the *c* direction. The modes of intermolecular overlapping are shown in Fig. 2. As shown, molecules A and C (B and D) adopt an eclipsed overlapping mode (Mode 1) with an intermolecular distance of 16 Å (the *c* parameter of the unit cell), while molecules C and F (D and E), F being inbetween A and C, overlap with a relative shift by approximately one TTF subunit along the long axis of the molecule and a slight shift along the short axis of the molecule (Mode 2). Molecules A, C and E are in the same lamina, while B, D and F form another lamina along the *a* direction.

Table 2 Bond lengths (Å) and selected angles (°) of BHBDTI in $[BHBDTI]_2[SiMo_{12}O_{40}]$

C(1)–C(2)	1.41(3)	C(2)–C(3)	1.40(3)
C(3)–C(4)	1.50(3)	C(5)–C(6)	1.46(2)
C(6)–C(7)	1.54(2)	C(7)–C(8)	1.45(3)
C(9)–C(10)	1.42(2)	C(11)–C(12)	1.39(2)
C(13)–C(18)	1.38(2)	C(13)–C(14)	1.43(2)
C(14)–C(15)	1.42(2)	C(15)–C(16)	1.41(2)
C(16)–C(17)	1.35(2)	C(17)–C(18)	1.40(2)
C(19)–C(20)	1.47(3)	C(20)–C(21)	1.42(3)
C(21)–C(22)	1.62(3)	C(22)–C(23)	1.35(3)
C(23)–C(24)	1.38(3)	C(25)–C(26)	1.45(2)
C(26)–C(27)	1.44(3)	C(27)–C(28)	1.60(3)
C(28)–C(29)	1.43(4)	C(29)–C(30)	1.45(3)
C(31)–C(32)	1.37(2)	C(33)–C(34)	1.35(2)
C(35)–C(36)	1.41(4)	C(36)–C(37)	1.47(3)
C(37)–C(38)	1.58(2)	C(39)–C(40)	1.46(2)
C(40)–C(41)	1.42(3)	C(41)–C(42)	1.46(3)
S(1)–C(10)	1.70(2)	S(1)–C(4)	1.85(2)
S(2)–C(9)	1.71(2)	S(2)–C(5)	1.85(2)
S(3)–C(11)	1.71(2)	S(3)–C(10)	1.73(2)
S(4)–C(9)	1.73(2)	S(4)–C(11)	1.75(2)
S(5)–C(12)	1.73(2)	S(5)–C(13)	1.738(14)
S(6)–C(12)	1.72(2)	S(6)–C(18)	1.736(14)
S(7)–C(31)	1.71(2)	S(7)–C(15)	1.726(13)
S(8)–C(31)	1.737(13)	S(8)–C(16)	1.759(14)
S(9)–C(32)	1.718(14)	S(9)–C(33)	1.73(2)
S(10)–C(32)	1.73(2)	S(10)–C(34)	1.741(13)
S(11)–C(33)	1.732(14)	S(11)–C(35)	1.85(4)
S(12)–C(34)	1.76(2)	S(12)–C(39)	1.80(2)
Cl(1)–C(30)	2.16(2)	Cl(2)–C(24)	2.19(3)
O(1)–C(17)	1.37(2)	O(1)–C(25)	1.43(2)
O(2)–C(14)	1.31(2)	O(2)–C(19)	1.40(2)
C(10)–S(1)–C(4)	103.5(8)	C(9)–S(2)–C(5)	102.0(8)
C(11)–S(3)–C(10)	96.5(8)	C(9)–S(4)–C(11)	95.9(7)
C(12)–S(5)–C(13)	94.2(8)	C(12)–S(6)–C(18)	94.3(7)
C(31)–S(7)–C(15)	95.4(7)	C(31)–S(8)–C(16)	95.4(7)
C(32)–S(9)–C(33)	97.0(7)	C(32)–S(10)–C(34)	96.0(7)
C(33)–S(11)–C(35)	100.8(12)	C(34)–S(12)–C(39)	104.1(7)
C(17)–O(1)–C(25)	115.3(11)	C(14)–O(2)–C(19)	119.1(13)
C(10)–C(9)–S(4)	115.6(11)	C(9)–C(10)–S(3)	116.1(12)
S(3)–C(11)–S(4)	115.9(8)	S(6)–C(12)–S(5)	117.6(9)
C(18)–C(13)–S(5)	116.7(11)	C(15)–C(14)–C(13)	115.3(13)
C(16)–C(15)–S(7)	117.9(10)	C(15)–C(16)–S(8)	114.1(10)
C(16)–C(17)–C(18)	116.6(14)	C(13)–C(18)–C(17)	122.3(13)
S(7)–C(31)–S(8)	117.2(8)	S(9)–C(32)–S(10)	113.9(7)
C(34)–C(33)–S(9)	116.4(11)	C(33)–C(34)–S(10)	116.6(11)

Table 3 Short intermolecular contacts (Å) in the group BCF

S(8F)···S(9C)	3.440	S(9F)···S(8C)	3.440
S(7F)···S(10C)	3.341	S(10F)···S(7C)	3.341
S(1C)···S(6B)	3.664	S(6C)···S(1B)	3.664
S(4C)···S(3B)	3.634	S(3C)···S(4B)	3.634
S(5C)···S(2B)	3.624	S(2C)···S(5B)	3.624

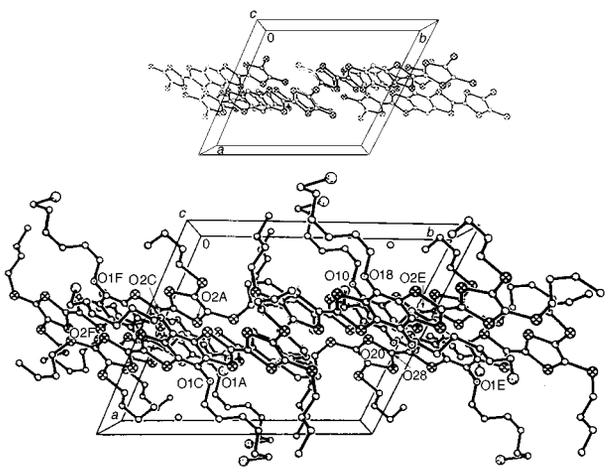

Fig. 2 Overlap patterns of the cations in $[BHBDTI]_2[SiMo_{12}O_{40}]$ along the *c* axis. Eight anions in corners are omitted for clarity as well as all alkyl and alkyloxy side-chains in the small diagram. Mode 1: eclipsed overlapping between A and C as well as B and D with an intermolecular distance of 16 Å. Mode 2: F and C overlap with a relative shift by about one TTF subunit along the long axis of the molecule and a slight shift along the short axis of the molecule, so do D and E.

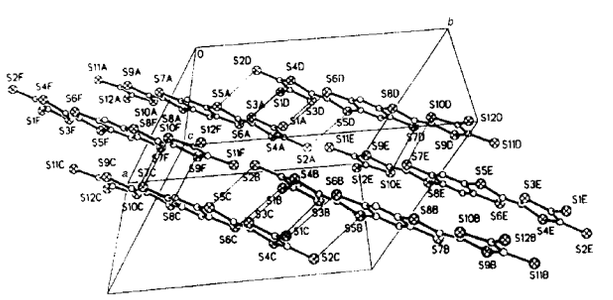

Fig. 3 The organic layer in the crystal structure of $[BHBDTI]_2[SiMo_{12}O_{40}]$. The dashed lines indicate S···S contacts shorter than 3.7 Å (alkyl and alkyloxy side-chains are omitted for clarity).

Figs. 3 and 4 show the stacks of the cations in different directions. The intermolecular short S···S contacts are also given in Fig. 3. As shown, the organic layer consists of two groups comprised of A, D, E and B, C, F, respectively, and divided by the (011) plane. The two groups ADE and BCF are related by the symmetry operation on the center of inversion 1/2, 1/2, 1/2. There is no short intermolecular contact between the groups, since the shortest interatomic distance is 4.365 Å between C(19A) and C(19F).

In each group, BHBDTI molecules are aligned in a head to tail manner along the [011] direction and overlap in the manner of Mode 2 along the *c* direction. Intermolecular S···S contacts shorter than the van der Waals value of 3.7 Å can be observed only within the groups, see Table 3 and Fig. 3, implying that the sulfur atom seems to play an important role for the formation of the groups and the steric effect of the alkyloxy side-chains prevents the two groups from closer packing. It is interesting that no S···S contact shorter than 3.6 Å is found in the crystal structure of the neutral molecule $C_{50}H_{84}O_2S_{12}$, which is a homologue of BHBDTI with a slight difference only in the alkyl side-chains.[13]

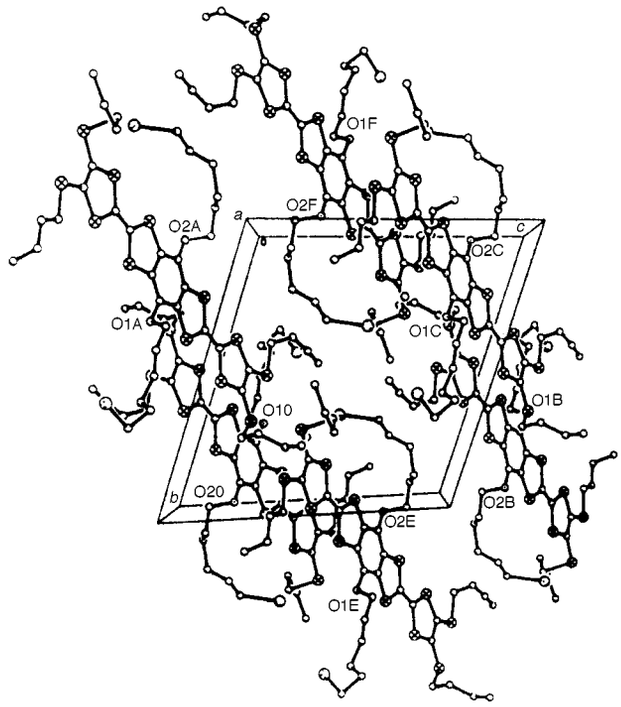

Fig. 4 The stacks of BHBDTI molecules along the *a* direction. The two isolated groups ADE and BCF which are related by the symmetry operation on the centre of inversion 1/2, 1/2, 1/2 are shown clearly divided by the (011) plane. There is no short intermolecular contact between them.

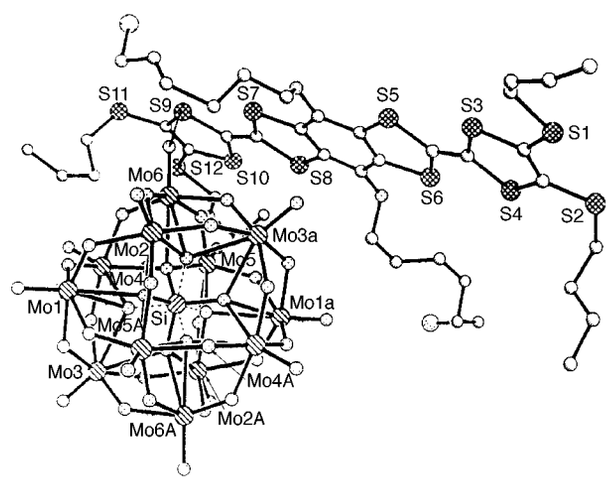

Fig. 5 A short contact between the BHBDTI dication and $[SiMo_{12}O_{40}]^{4-}$ anion. The thin line between S9 and O3 indicates the shortest S···O distance (3.036 Å).

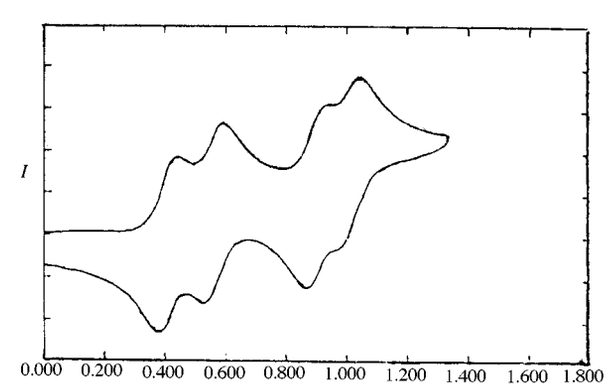

Fig. 6 Cyclic voltammogram for BHBDTI (CH_2Cl_2, NBu_4PF_6, 100 mV s^{-1}, −20 °C).

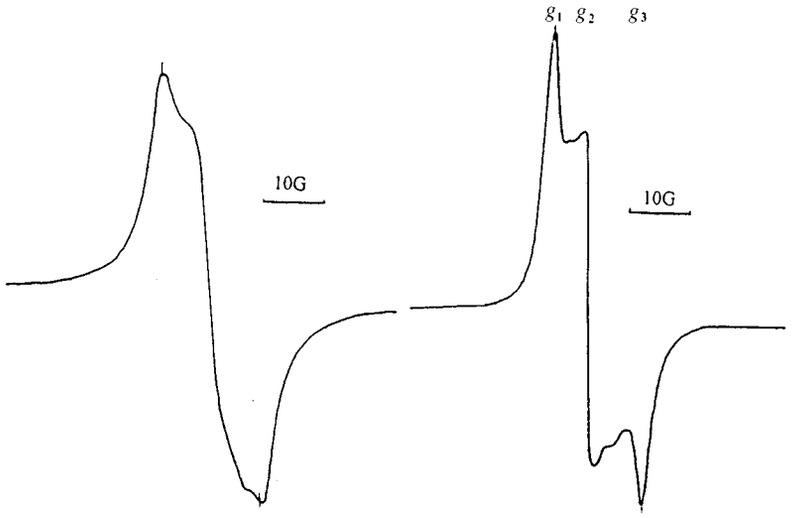

Fig. 7 The ESR spectra of $[C_{42}H_{60}Cl_2O_2S_{12}]_2[SiMo_{12}O_{40}]$ at r.t. (left) and 77 K (right).

The presence of a short contact between the organic and inorganic layers through the S atom and terminal O atom of the polyoxoanion with the shortest S···O distance of 3.036 Å is also observed, see Fig. 5. All these results led us to conclude that van der Waals interaction through S···S and S···O contacts favors the formation of 1-D conducting layers, but the long alkyl and alkyloxy side-chains prevent the conducting layer from extension.

Physical properties

(a) IR spectrum. The IR spectrum of the present compound is similar to those of other sulfur containing radical-cation salts. A very broad band appears at 3500–4000 cm^{-1} usually attributed to charge-transfer transitions within the donors. The bands arising from the polyoxoanion in the range 1000–600 cm^{-1} remain unchanged.[21] The bands appearing in the vibronic region of 1400–1000 cm^{-1} change slightly either in intensities or in positions compared with those of BEDT-TTF salts.

(b) Cyclic voltammogram. The cyclic voltammetric behavior of BHBDTI indicates that it belongs to Class 4, according to the classification by Müllen and co-workers,[22] *i.e.* intramolecular effects between TTF subunits of the donor result in distinct one-electron transfer processes, see Fig. 6. The charging up to a tetracation occurs at *ca.* 600 mV. However, $\Delta E^3_{\frac{1}{2}}$ (340 mV) between the second and the third oxidation steps is about 200 mV higher than those between the first and second (150 mV) or the third and the fourth steps (100 mV). Further, the redox potential for the third oxidation step ($E^3_{\frac{1}{2}}$) is found to be 160 mV higher than that for the second step ($E^2_{\frac{1}{2}}$) of "mono" TTF compounds which is due to an increased repulsion energy between the doubly charged moiety and the singly-charged part of the "dimers". The polarographic half wave potentials for the anion, α-$SiMo_{12}$, were $E^1_{\frac{1}{2}} = +250$ (2e), $E^2_{\frac{1}{2}} = +130$ (2e) and $E^3_{\frac{1}{2}} = -60$ mV (2e), in 0.5 mol L^{-1} HCl, 50% water–alcohol, *vs.* SCE. The redox potentials will be lower in organic solvents. The polarographic results for both the inorganic and the organic precusors support the present formulation and dication of BHBDTI present in the hybrid molecule.

(c) XPS spectra. X-Ray photoelectron spectroscopy revealed the stoichiometric ratio S : O = 24 : 44, in agreement with the molecular formula. The electron binding energy of S_{2p} is 163.9 eV with the full width at half maximum > 2.0 eV suggesting the presence of sulfur atoms with different oxidation states.

(d) EPR spectra. The EPR spectra were measured at r.t. and at 77 K, see Fig. 7. It shows significant anisotropy in g with values of 2.009, 2.006 and 2.000 and still no molybdenum(v) signal at 77 K. We assume that the anion is diamagnetic and therefore the signals are due only to the presence of spins localized in BHBDTI radical dications.

(e) d.c. Conductivity. The electric conductivity was measured at room temperature on powder samples by the two-contact method to give $\rho_{r.t.} = 1.3 \times 10^{-4}$ S cm^{-1} indicating that the compound is a semiconductor. This is an interesting result, since the d.c. electrical conductivity seems too high for that expected for a single-valence compound of "mono" TTF.

Experimental

Preparation of $[C_{42}H_{60}Cl_2O_2S_{12}]_2[SiMo_{12}O_{40}]$ crystals

2,6-[4,5-Bis(*n*-butylsulfanyl)-1,3-dithiol-2-ylidene]-4,8-bis(6-iodo-*n*-hexyloxy)-1,3,5,7-tetrathia-s-indacene (BHBDTI) was prepared by the method of Adam *et al.*[22,23] The salt $[NBu_4]_4[SiMo_{12}O_{40}]$ was prepared according to the literature;[24] $[C_{42}H_{60}Cl_2O_2S_{12}]_2[SiMo_{12}O_{40}]$, $[BHBDTI]_2[SiMo_{12}O_{40}]$, was synthesized by a similar method.[25] Crystals of the latter were obtained on a platinum wire electrode by anodic oxidation of BHBDTI in the electrocrystallization cell under low constant current ($I = 1.0$ μA cm^{-2}) in the presence of the $[NBu_4]_4[SiMo_{12}O_{40}]$ (4.5×10^{-3} M) as supporting electrolyte. The solvent was $CHCl_2CH_2Cl$–CH_3CN (1 : 1). Some water was added to the anodic compartment of the cell at the beginning of electrolysis. By this method, we were able to obtain black plate single crystals of good quality. In other cases, only long brown fibrous substances which we did not try to identify grew on the anode (Found: C, 24.8; H, 2.8; S, 22.5. $[C_{42}H_{60}Cl_2O_2S_{12}]_2[SiMo_{12}O_{40}]$ requires C, 25.7; H, 3.1; S, 19.6%). $\tilde{\nu}_{max}/cm^{-1}$ 2940sh, 2916s, 2854s, 1392vs, 1342s, 1262s, 1192sh, 1050m, 1021w, 944s, 900vs, 865sh, 794vs (KBr).

Cyclic voltammetry

The cyclic voltammogram of BHBDTI was obtained in CH_2Cl_2, NBu_4PF_6, at 100 mV s^{-1}, *vs.* SCE. Four half wave potentials for the oxidation of BHBDTI were $E^1_{\frac{1}{2}}$, +410, $E^2_{\frac{1}{2}}$, +560, $E^3_{\frac{1}{2}}$, +300 and $E^4_{\frac{1}{2}}$, +1000 mV, each corresponding to a one-electron step.

X-Ray crystallographic determination

Crystal data. $C_{84}H_{120}Cl_4Mo_{12}O_{44}S_{24}Si$, $M = 3924.41$, triclinic, space group $P\bar{1}$, $a = 15.088(3)$, $b = 16.416(3)$, $c = 16.675(3)$ Å, $U = 3338.9(12)$ Å^3, $T = 293$ K, $Z = 1$, μ(Mo-K$_\alpha$) = 1.6 mm^{-1}, 13408 reflections measured, 11552 independent ($R_{int} = 0.0204$).

The final $wR(F^2)$ was 0.2811, $R1 = 0.0924$. The residuals were 5.128 and -2.157 e Å^{-3} for the maximum peak and hole respectively. The large values of the residuals may arise from the disorder of the anion, which is common in salts of this type, or of solvent molecules, which cannot be located.

CCDC reference number 186/1176.

See http://www.rsc.org/suppdata/dt/1998/3865/ for crystallographic files in .cif format.

Physical measurements

The IR spectrum was recorded on a FTS-7 spectrophotometer, XPS spectra on a VG-ESCA LAB-Mk II electrophotometer and X-band EPR spectra on a TES-FE-3AX spectrometer. The electric conductivity was measured by the two-contact method.[26] The elemental analyses were carried on a MOD 1106 elemental analyzer.

Acknowledgements

J. Peng wishes to thank Professor R.-Y. Zhan for helpful discussion on the EPR results. This project was supported by the National Natural Science Foundation of China.

References

1 M. T. Pope and A. Müller, *Polyoxometalates: From Platonic Solids to Antiretroviral Activity*, Kluwer, Dordrecht, 1994.
2 C. L. Hill (Editor), *Chem. Rev.*, 1998, **98** and refs. therein; E. B. Wang, C. W. Hu and L. Xu, *Concise polyoxometalates*, Chemical Industry, Beijing, 1997.
3 J. Ferraris, D. O. Cowan, V. J. Walatka and J. H. Perlstein, *J. Am. Chem. Soc.*, 1973, **95**, 948.
4 J. M. Williams, A. J. Schultz, U. Geiser, K. D. Carlson, A. M. Kini, H. H. Wang, W.-K. Kwok, M.-H. Whangbo and J. E. Schirber, *Science*, 1991, **252**, 1501.
5 J. M. Williams, J. R. Ferraro, R. J. Thorn, K. D. Carlson, U. Geiser, H. H. Wang, A. M. Kini and M. H. Wangbo, *Organic Superconductors*, *Synthesis*, *Structure Properties and Theory*, ed. R. N. Grimes, Prentice Hall, Englewood Cliffs, NJ, 1992.
6 M. Adam and K. Müllen. *Adv. Mater.*, 1994, **6**, 439.
7 A. Davidson, K. Boubekeur, A. Pénicaud, P. Auban, C. Lenoir, P. Batail and G. Hervé, *J. Chem. Soc.*, *Chem. Commun.*, 1989, 1373.
8 C. Bellitto, M. Bonamico, V. Fares, F. Federici and G. Righini, *Chem. Mater.*, 1995, **7**, 1475.
9 L. Ouahab, *Chem. Mater.*, 1997, **9**, 1909 and refs. therein.
10 E. Coronado and C. J. Gómez-García, *Chem. Rev.*, 1998, **98**, 273 and refs. therein.
11 E. Coronado, J. R. Galán-Mascarós, C. Giménez-Saiz, C. J. Gómez-García and V. N. Laukhin, *Adv. Mater.*, 1996, **8**, 801.
12 S. Triki, L. Ouahab, D. Grandjean, R. Canet, C. Garrigou-Lagrange and P. Delhaes, *Synth. Met.*, 1993, **55–57**, 2028.
13 S. Frenzel and K. Müllen, *Synth. Met.*, 1996, **80**, 175.
14 P. Le Magueres, L. Ouahab, S. Golhen, D. Grandjean, O. Pena, J.-C. Jegaden, C. J. Gómez-García and P. Delhaes, *Inorg. Chem.*, 1994, **33**, 5180.
15 R. Neier, C. Trojanowski and R. Mattes, *J. Chem. Soc.*, *Dalton Trans.*, 1995, 2521.
16 V. A. Sergienko, M. A. Porai-Koshits and E. N. Yurchenko, *Zh. Struct. Khim.*, 1980, **21**, 111; *J. Struct. Chem.* (*Engl. Transl.*), 1980, **21**, 87.
17 J. Fuchs, A. Tiele and R. Palm, *Angew. Chem.*, *Int. Ed. Engl*,. 1982, **23**, 789.
18 H. T. Evans and M. T. Pope, *Inorg. Chem.*, 1984, **23**, 501.
19 J. Peng, Ph. D. Thesis, Northeast Normal University. 1997.
20 H. Ichida, A. Kobayashi and Y. Sasaki, *Acta Crystallogr.*, *Sect. B*, 1980, **36**, 1382.
21 C. Rocchiccioli-Detcheff, M. Fournier, R. Franck and R. Thouvenot, *Inorg. Chem.*, 1983, **22**, 207.
22 M. Adam, U. Scherer, Y. J. Shen and K. Müllen, *Synth. Met.*, 1992, **55–57**, 2108.
23 U. Scherer, Y. J. Shen, M. Adam, W. Bietsch, J. U. von Schutz and K. Müllen, *Adv. Mater.*, 1993, **5**, 109.
24 C. Sanchez, J. Livage, J. P. Launay, M. Fournier and Y. J. Jeannin, *J. Am. Chem. Soc.*, 1982, **104**, 3195.
25 C. J. Gómez-García, G.-S. Carlos, S. Triki, E. Coronado, P. L. Magueres, L. Ouahab, L. Ducasse, C. Sourisseau and P. Delhaes, *Inorg. Chem.*, 1995, **34**, 4139.
26 F. Wudl and M. R. Bryce, *J. Chem. Educ.*, 1990, **87**, 717.

Paper 8/04934C